iScience, Volume *27*

Supplemental information

Nox4-SH3YL1 complex is involved in diabetic nephropathy

Sae Rom Lee, Hye Eun Lee, Jung-Yeon Yoo, Eun Jung An, Soo-Jin Song, Ki-Hwan Han, Dae Ryong Cha, and Yun Soo Bae

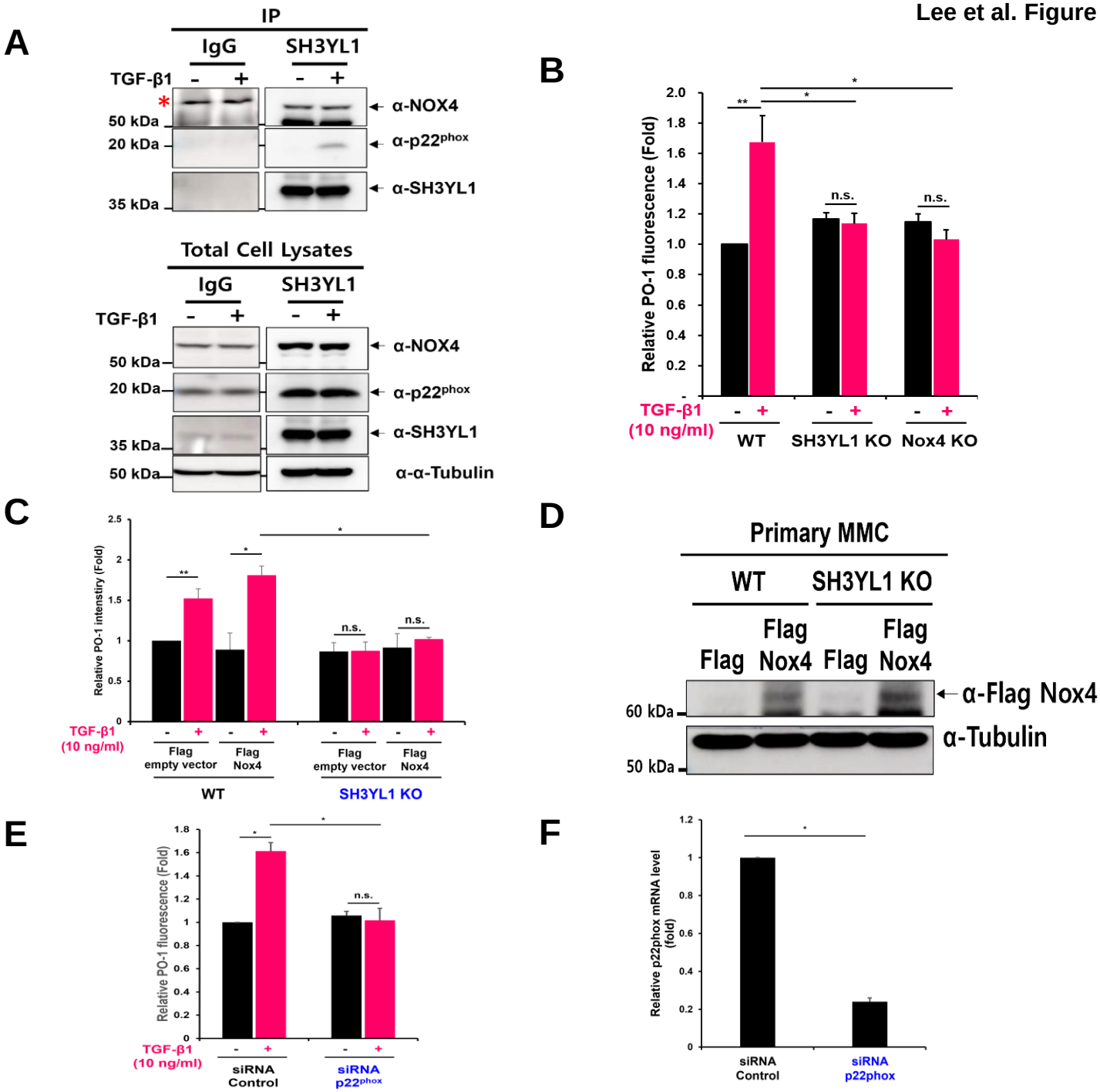

Figure S1. SH3YL1 interacts with Nox4-p22^{phox} complex and stimulates Nox4-dependent H_2O_2 generation in kidney mesangial cells related to Figure 1. (A) Mouse primary mesangial cells (pMMC) were incubated with TGF-β1 (10 ng/ml) for 30 min and then the pMMC lysates were treated with SH3YL1 antibody for the co-IP assay. The resulting precipitates were immunoblotted with the indicated antibodies. Red asterisk means nonspecific band. (B) Isolated pMMCs from WT, SH3YL1, and Nox4 KO mice were serum starved for 6 h and stimulated with TGF-β1 (10 ng/ml) in the presence of 5 μM of PO-1 for 10 min in the dark at 37 ℃. The H_2O_2 generation shown as PO-1 fluorescence, was monitored by confocal microscopy. Four to five fields of cells were randomly selected, and the mean intensity was obtained using LSM 880 software (N = 3, data shown as mean ± SD, *p < 0.005, **p < 0.05 as determined by the Student's t-test). (C) pMMCs from WT, SH3YL1 KO mice were transiently overexpressed with Flag-Nox4. The cells were serum-starved overnight and stimulated with TGF-β1 (10 ng/ml) with 5 μM of PO-1 for 10 min. Four to five fields were randomly obtained from LSM-880 software (N=3, data shown as mean ± SD, *p<0.005, **p<0.05 as determined by students t-test). (D) The flag-Nox4 expressions were analyzed by immunoblotting using antibody against Flag. (E) pMMCs were transfected with control or p22^{phox} siRNA for overnight and the hydrogen peroxide generation was monitored using PO-1 by confocal microscopy. Four to five fields were randomly obtained from LSM-880 software (N=3, data shown as mean ± SD, *p<0.005, **p<0.05 as determined by students t-test). (F) The p22^{phox} mRNA expressions were analyzed by real-time PCR.

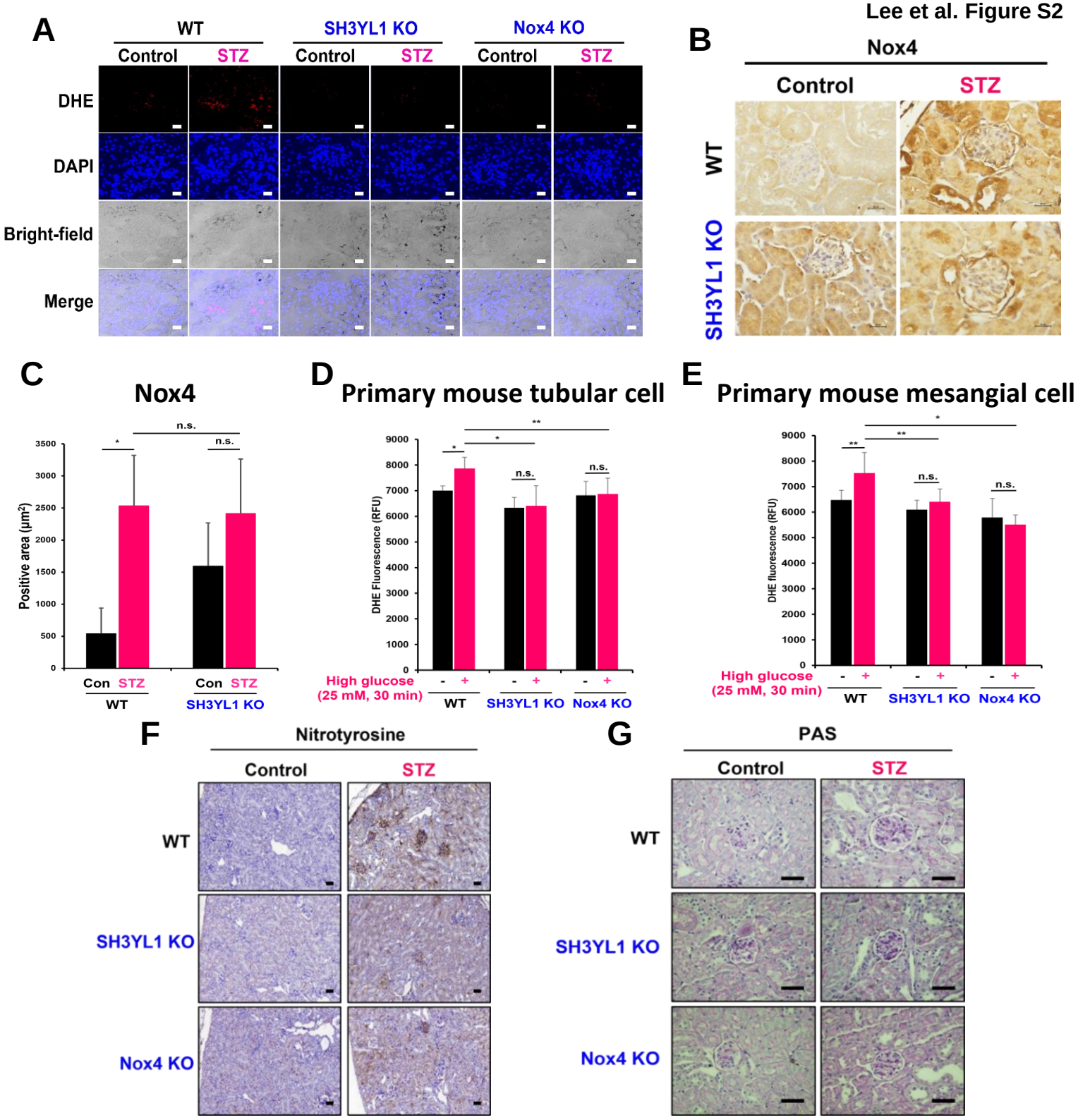

Figure S2. Deficiency of SH3YL1 ameliorates oxidative stress and diabetic kidney damage, related to Figure 1. WT, SH3YL1 and Nox4 KO mice were divided into two groups of control or STZ-injected mice. (A) Frozen section of kidney tissues (10 μm) were stained with DHE for ROS detection. (400X, scale bar = 20 μm). (B) IHC staining with antibody against Nox4. The positive areas turned brown with DAB application (600X, scale bar = 20 μm). (C) Quantification of Nox4 positive areas. Fields (10 - 15) were analyzed with Image-Pro Plus 7 (N = 5 - 7 per group, data shown as mean ± SD, *p < 0.005, **p < 0.05 as determined by the Student's t-test). (D) , (E) Primary mouse tubular cells or primary mouse mesangial cells from WT, SH3YL1, and Nox4 KO mice were were treated with 25 mM of high glucose after 3 hrs of serum starvation. DHE level was assayed using DHE kit according to the manufacturer's protocol. (N = 4 – 6 per group, data shown as mean ± SD, *p < 0.005, **p < 0.05 as determined by the Student's t-test). (F) IHC staining with antibody against nitrotyrosine. The positive areas turned brown with DAB application (200X, scale bar = 50 μm). (G) The kidney sections were PAS-stained to see mesangial expansion. Glomeruli images (26 - 30) were taken by microscopy (Nikon, DS/F3, 400X, scale bar = 50 μm).

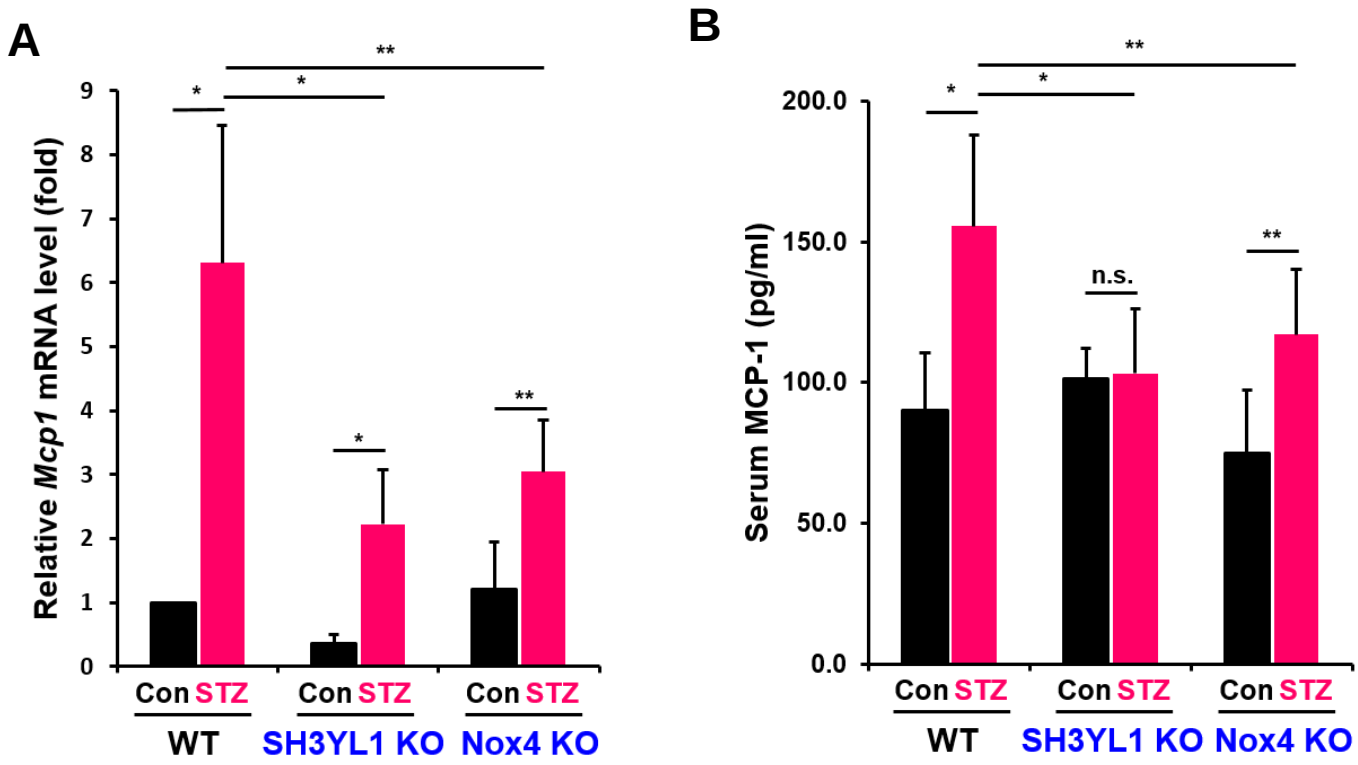

Figure S3. SH3YL1 deficiency attenuates MCP-1 level in STZ injected mice, related to Figure 2. (A) RNA from frozen kidney tissue were analyzed for Mcp1 expression. Real-time PCR with each primer and the results were normalized with 18S (N = 5-8 per group, data shown as mean ± SD, *p<0.005, **p<0.05 as determined by student's t-test). (B) Mouse serum from control and STZ injected group from WT, SH3YL1 or Nox4 KO mice were measured for MCP-1 level using ELISA kit (N = 5-6 of per group, data shown as mean ± SD, *p<0.005, **p<0.05 as determined by student's t-test).

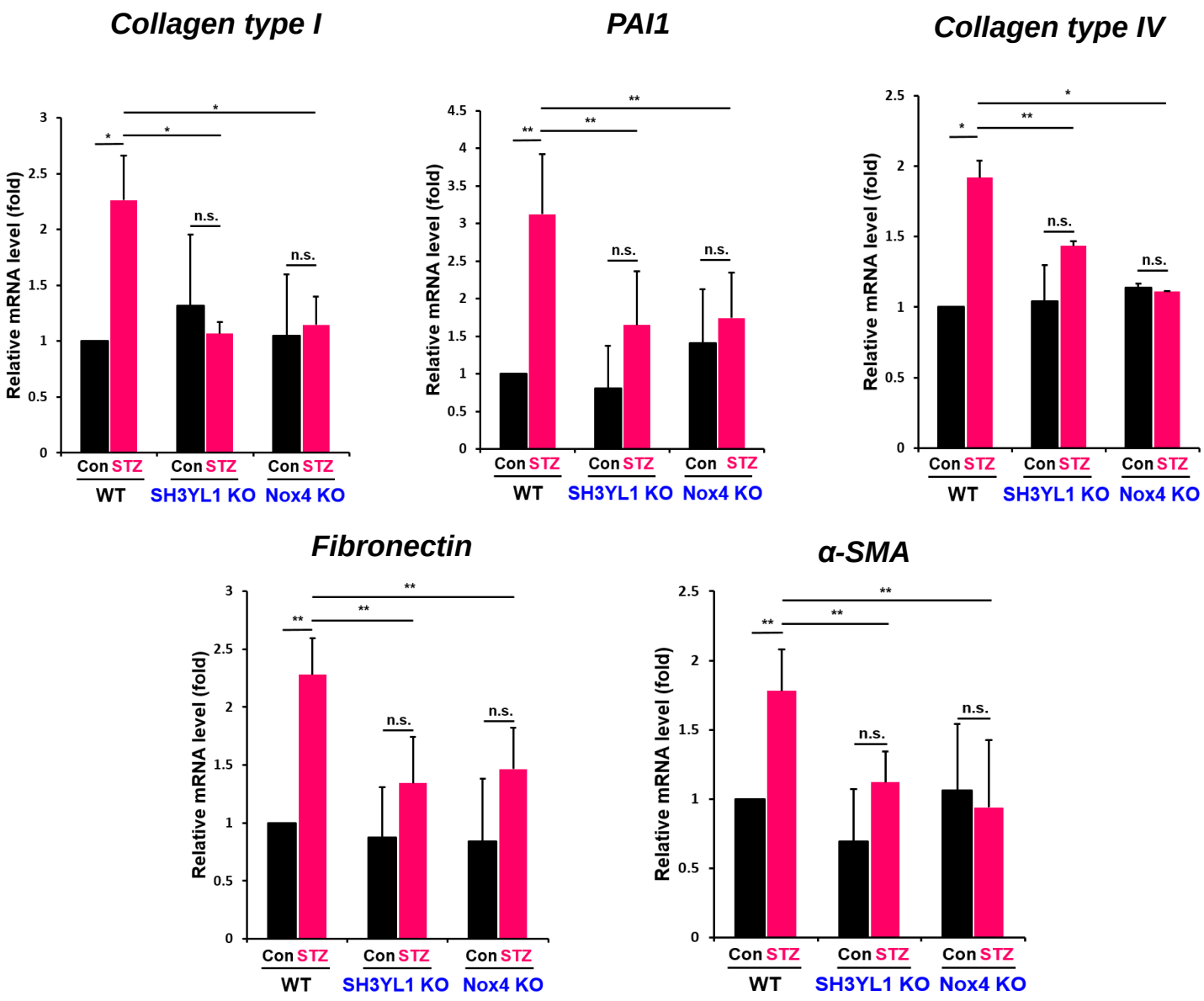

Figure S4. Fibrotic markers are reduced in diabetic SH3YL1 and Nox4 KO mice, related to Figure 2. Snap frozen kidney tissues were RNA extracted from each group. Total RNA extractions of kidney tissue were reverse transcribed and real-time PCR was performed with indicated primers in 'Table S5'. Quantification of Collagen type I, PAI1, Collagen type IV, fibronectin (Fn) and α-smooth muscle actin (α-SMA) mRNA expression. The results were normalized by 18s (N = 5-9 per group, data shown as mean ± SD, *p<0.005, **p<0.05 as determined by student's t-test).

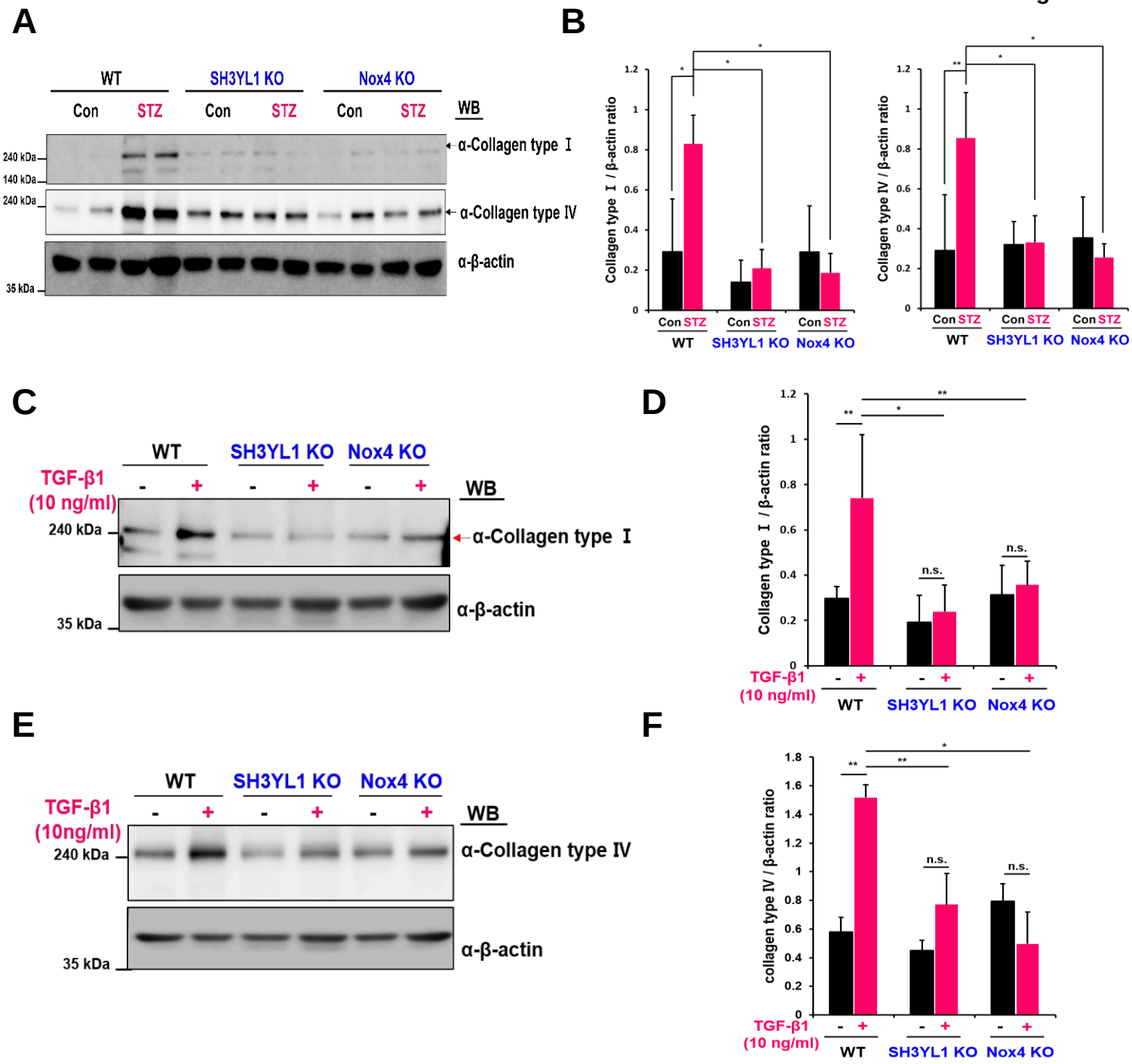

Figure S5. Collagen expressions are attenuated in diabetic SH3YL1 and Nox4 KO mice kidney, related to Figure 2. Snap frozen kidney tissues were protein extracted from each group. (A) Immunoblot of kidney tissue and antibodies against Collagen type Ⅰ or Ⅳ. (B) The western blot was quantified using Image J (N = 3-4 of mice per group, data shown as mean ± SD, *p<0.005, **p<0.05 as determined by student's t-test). Primary mouse mesangial cells (pMMCs) were treated with TGF-β1 (10 ng/ml) and harvested after 24 hrs and lysed. The collagen type Ⅰ (C) or Ⅳ (E) was analyzed by immunoblotting with Collagen type Ⅰ or Ⅳ antibody. Immunoblots of Collagen type Ⅰ (D) or Ⅳ (F) quantification by using Image J (N = 3, data shown as mean ± SD; *P<0.005, **P<0.05 as determined by student's t-test).

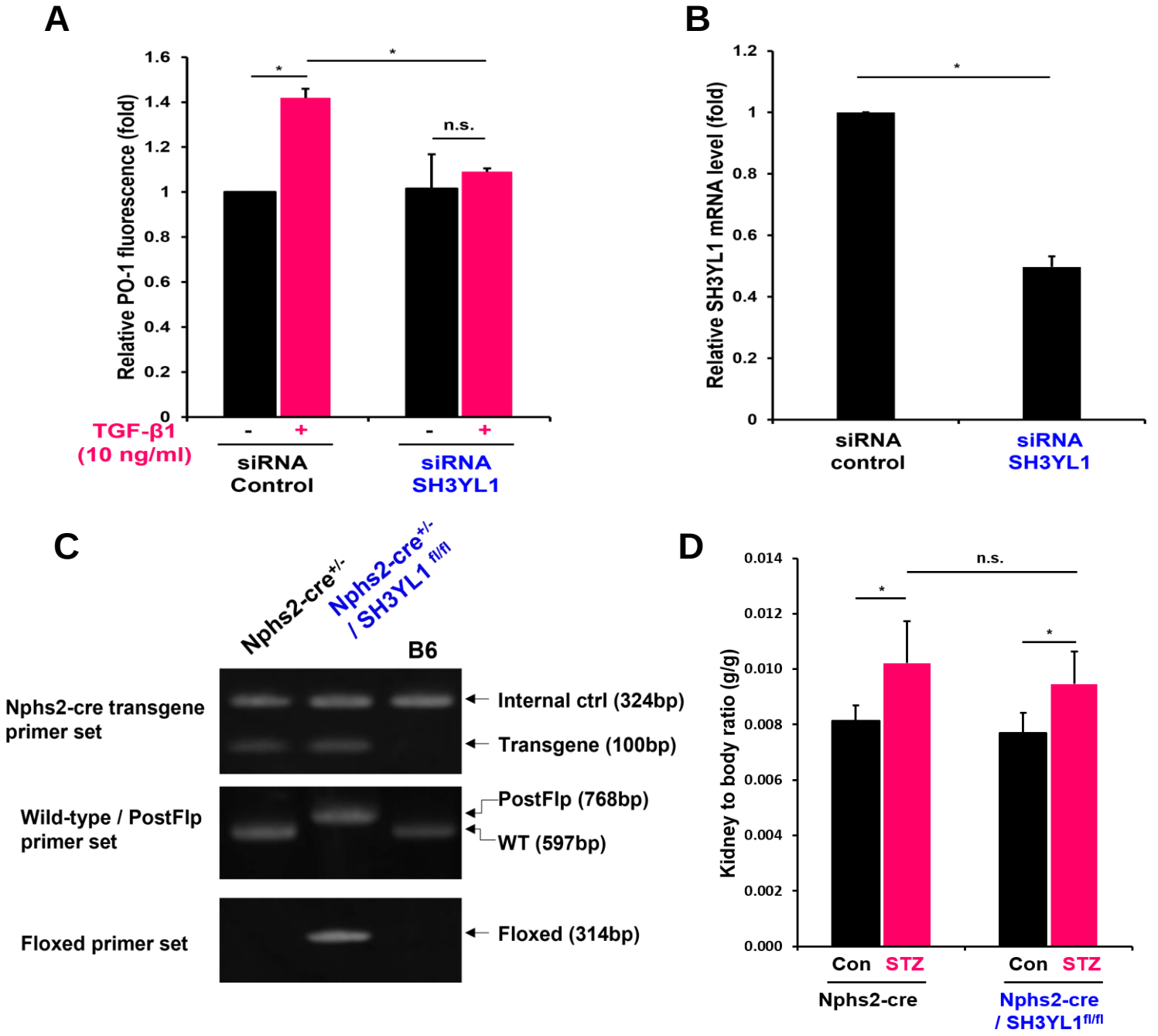

Figure S6. Function of SH3YL1 in TGFβ1-mediated H_2O_2-generation in MPC, related to Figure 3, 4 and 5. (A) Mouse podocytes (MPCs) were transfected with SH3YL1 siRNA for overnight and stimulated with TGF-β1 (10 ng/ml) with PO-1 for 10 min. Four to five fields of the cells were randomly selected and PO-1 intensity was obtained from the LSM 880 software (N=3, data shown as mean ± SD, *p<0.005, **p<0.05 as determined by students t-test). (B) Knock-down of SH3YL1 was analyzed by real-time PCR. (C) Genotyping of podocyte-specific deletion of SH3YL1 compared to Nphs2-Cre$^{+/-}$ with Nphs2-Cre$^{+/-}$/SH3YL1$^{fl/fl}$ mice. Detail genotyping information is in the 'Star Methods' (D) Left kidney was isolated and weighted for kidney-to-body weight ratio (g/g) (N = 10 per group, *P<0.005, **P<0.05, n.s. represents not significant, as determined by student's t-test)

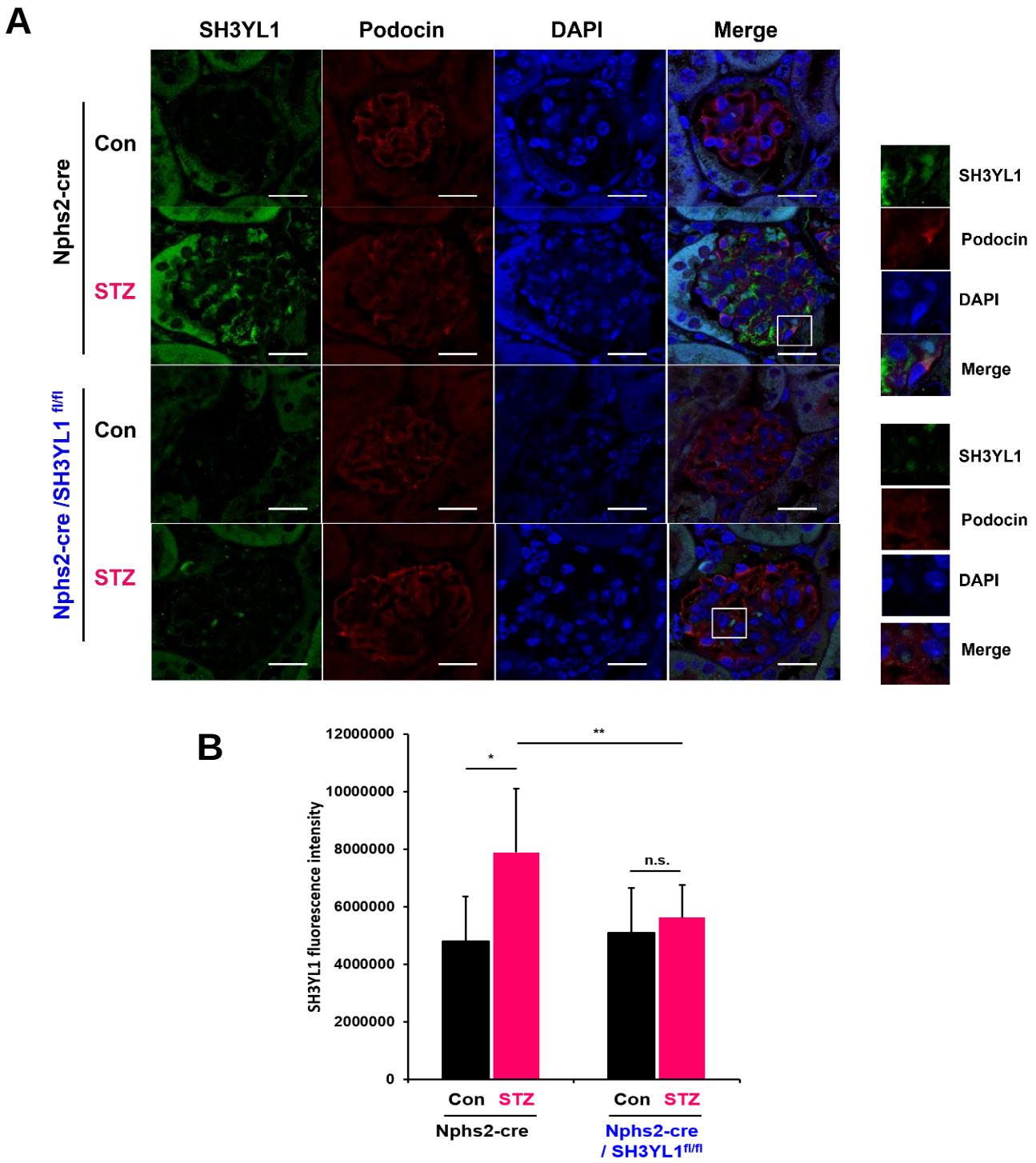

Figure S7. SH3YL1 expression is increased in the diabetic kidney tissue, related to Figure 7. (A) Immunofluorescence staining of SH3YL1 with podocyte specific marker, Podocin in the paraffin-embedded kidney section from Nphs2-Cre or Nphs2-Cre/SH3YL1$^{fl/fl}$ mice. (B) Images were taken by a confocal microscopy (LSM880 airyscan). Magnification for SH3YL1 (960X, scale bar = 20 μm). 6 to 7 glomeruli of each sample were analyzed with Image J (N = 7-8 for each group, data shown as mean ± SD, *p<0.005, as determined by student's t-test).

Table S1. Fasting blood glucose monitoring in STZ-induced type Ⅰ diabetic mouse model, related to Figure 1.

Weeks	0	4	8	12
WT-Con	174±20	167±27	158±28	150±17
WT-STZ	172±12	508±111*	527±76*	542±64*
SH3YL1 KO-Con	155±12	164±25	155±20	158±21
SH3YL1 KO-STZ	154±14	463±98*	455±75*	500±69*
Nox4 KO-Con	158±24	166±22	168±29	156±37
Nox4 KO-Con	175±30	531±61*	571±56*	587±21*

Fasting blood glucose (mg/dl) was monitored every 4 weeks from tip of the tail and mice with over 300 mg/dL of blood glucose were considered diabetic. (N = 7-8 per group, data shown as mean ± SD, *P<0.005 vs control mice, as determined by student's t-test).

*P<0.005 vs respective control mice

Table S2. Blood pressure (mmHg) (BP, systolic, diastolic and mean value) and kidney-to-body weight ratio, related to Figure 1.

	WT		SH3YL1 KO		Nox4 KO	
	Con	STZ	Con	STZ	Con	STZ
Systolic BP (mmHg)	130.2±8.7	132.7±25.7	111.7±7.9**	111.0±27.3	116.3±14.3	151.2±10.8
Diastolic BP (mmHg)	100.4±7.5	87.2±37.1	74.4±7.4**	71.6±28.5	82.4±11.5	94.9±3.7
Mean BP (mmHg)	110.0±7.6	102.0±33.2	86.6±5.5**	84.4±27.9	93.4±12.4	113.4±6.1
KW / BW	0.008±0.001	0.011±0.003*	0.008±0.001	0.009±0.001**	0.008±0.001	0.010±0.001 n.s.

The systolic, diastolic and mean blood pressure were measured using noninvasive tail-cuff system (N=2-5 per group, data are as mean s± SD, * P<0.005, ** P<0.05 vs WT-Control). Left kidney was isolated and weighted for kidney to body weight ratio (g/g) (N = 8-9 per group, *P<0.005, **P<0.05, n.s. represents not significant, as determined by student's t-test)

BP, Blood pressure; KW / BW: Kidney-to-body weight ratio

Table S3. Fasting blood glucose monitoring in STZ-induced type Ⅰ diabetes of Nphs2-Cre or Nphs2-Cre/SH3YL1$^{fl/fl}$ mice, related to Figure 4.

Weeks	0	4	8	12
Nphs2-Cre_Con	177±38	153±17	139±9	152±13
Nphs2-Cre_STZ	164±14	495±69*	505±52*	493±54*
Npsh2-Cre /SH3YL1 fl/fl_Con	174±14	150±18	156±22	158±13
Npsh2-Cre /SH3YL1 fl/fl_STZ	173±19	495±67*	509±80*	492±51*

Mice from Nphs2-Cre or Nphs2-Cre/SH3YL1$^{fl/fl}$ were divided into two groups; control and STZ injected groups. STZ was injected for five constitutive days with 50 mg/kg and fasting blood glucose level was monitored every four weeks in the blood from tip of the tail. (N = 10, data shown as mean ± SD, *p<0.005 compared to each control group, as determined by student's t-test).

STZ, Streptozotocin; fl/fl, floxed/floxed

Table S4. Clinical characteristics of study population, related to Figure 7.

Clinical parameters	Control	DN patients	P value
male/female	7/9	12/11	
Age (years)	37.5±6.6	55.6±11.0	<0.001
Body weight (g)	65.7±11.5	73.9±14.6	0.070
BMI	25.8±4.0	26.6±4.5	0.580
SBP (mmHg)	115±7	127±10	<0.001
DBP (mmHg)	72±7	78±8	0.024
Hb (g/dL)	13.6±1.5	13.8±1.2	0.720
BUN (mg/dL)	13.3±4.1	20.2±9.5	0.004
Creatinine (mg/dL)	0.70±0.30	1.19±0.59	0.001
eGFR (ml/min/m2)	104.6±10.1	68.1±28.6	<0.001
Serum protein (g/dL)	7.2±0.3	7.0±0.4	0.143
Serum albumin (g/dL)	4.6±0.2	4.3±0.3	0.014
Cholesterol (mg/dL)	164±32	180±42	0.200
LDL-cholesterol (mg/dL)	98±34	109±42	0.386
Triglyceride (mg/dL)	126±57	162±105	0.221
Uric acid (mg/dL)	4.9±1.4	6.0±1.8	0.046
FBS (mg/dL)	95±9	138±41	<0.001
Hba1C (%)	N.A.	6.69±0.79	
Urine PCR (mg/gCr)	120±87	1354±942	<0.001

BMI, body mass index; SBP, systolic blood pressure; DBP, diastolic blood pressure; BUN, blood urea nitrogen; eGFR, estimated glomerular filtration rate; FBS, fasting blood glucose, Urine PCR, urine protein/creatinine ratio; DN, Diabetic nephropathy

Table S5: Oligonucleotides used in this work, related to STAR Methods.

Name	Sequences (5'-3')	Ref
Mouse Collagen type Ⅰ (a2) (Col1a2) F	TCAAGGTCTACTGCAACATGG	[S1]
Mouse Collagen type Ⅰ (a2) (Col1a2) R	TGTAGGTGAAGCGACTGTTG	[S2]
Mouse Collagen type Ⅳ (a1) (Col4a1) F	GCCTTCCGGGCTCCTCAG	[S3]
Mouse Collagen type Ⅳ (a1) (Col4a1) R	TTATCACCAGTGGGTCCG	[S3]
Mouse Plasminogen activator inhibitor-1 (Pai1) F	TCCTCATCCTGCCTSSGTTCT	[S4]
Mouse Plasminogen activator inhibitor-1 (Pai1) R	GTGCCGCTCTCGTTTSCCTC	[S4]
Mouse Fibronectin (Fn) F	GGTTTCCCATTACGCCATTG	[S5]
Mouse Fibronectin (Fn) R	ATTCTCCCTTTCCATTCCCG	[S5]
Mouse α-smooth muscle actin(α-SMA) (Acta2) F	TCAGCGCCTCCAGTTCCT	[S6]
Mouse α-smooth muscle actin(α-SMA) (Acta2) R	AAAAAAAACCACGAGTAACAA ATCAA	[S6]
Mouse Monocyte chemotactic protein-1 (Mcp1) F	CTTCTGGGCCTGCTGTTCA	[S7]
Mouse Monocyte chemotactic protein-1 (Mcp1) R	CCAGCCTACTCATTGGGATCA	[S7]
Mouse 18S ribosomal RNA (18s) F	AGGAATTGACGGAAGGGCAC CA	This lab
Mouse 18S ribosomal RNA (18s) R	GTGCAGCCCCGGACATCTAA G	This lab
Transgene F	GCG GTC TGG CAG TAA AAA CTA TC	stock # 008205 Jackson Laboratories
Transgene R	GTG AAA CAG CAT TGC TGT CAC TT	stock # 008205 Jackson Laboratories
Internal control F	CTA GGC CAC AGA ATT GAA AGA TCT	stock # 008205 Jackson Laboratories
Internal control R	GTA GGT GGA AAT TCT AGC ATC ATC C	stock # 008205 Jackson Laboratories
CSD-loxF	GAG ATG GCG CAA CGC AAT TAA TG	[S8]
CSD- SH3YL1-F	TGA GGT ATG TTC TGT GCT GAG ACC C	[S8]
CSD-SH3YL1-R	TCA CAT GGA GGT GCT ATA GAA GGG C	[S8]
CSD- SH3YL1-ttR	CTT TGC GTA GAT AAG GCC AGA AGC C	[S8]
CSD-neo-F primer	GGGATCTCATGCTGGAGTTCT TCG	[S8]

Supplemental Reference

[S1]. Timmers, L., van Keulen, J.K., Hoefer, I.E., Meijs, M.F., van Middelaar, B., den Ouden, K., van Echteld, C.J., Pasterkamp, G., and de Kleijn, D.P. (2009). Targeted deletion of nuclear factor kappaB p50 enhances cardiac remodeling and dysfunction following myocardial infarction. Circ Res *104*, 699-706. 10.1161/CIRCRESAHA.108.189746.

[S2]. Kang, K.R., Kim, J.S., Seo, J.Y., Lim, H., Kim, T.H., Yu, S.K., Kim, H.J., Kim, C.S., Chun, H.S., Park, J.C., and Kim, D.K. (2022). Nicotinamide phosphoribosyltransferase regulates the cell differentiation and mineralization in cultured odontoblasts. Korean J Physiol Pharmacol *26*, 37-45. 10.4196/kjpp.2022.26.1.37.

[S3]. Castro, N.E., Kato, M., Park, J.T., and Natarajan, R. (2014). Transforming growth factor beta1 (TGF-beta1) enhances expression of profibrotic genes through a novel signaling cascade and microRNAs in renal mesangial cells. J Biol Chem *289*, 29001-29013. 10.1074/jbc.M114.600783.

[S4]. Kang, Y.S., Song, H.K., Lee, M.H., Ko, G.J., Han, J.Y., Han, S.Y., Han, K.H., Kim, H.K., and Cha, D.R. (2010). Visfatin is upregulated in type-2 diabetic rats and targets renal cells. Kidney Int *78*, 170-181. 10.1038/ki.2010.98.

[S5]. Sancho, P., Mainez, J., Crosas-Molist, E., Roncero, C., Fernandez-Rodriguez, C.M., Pinedo, F., Huber, H., Eferl, R., Mikulits, W., and Fabregat, I. (2012). NADPH oxidase NOX4 mediates stellate cell activation and hepatocyte cell death during liver fibrosis development. PLoS One *7*, e45285. 10.1371/journal.pone.0045285.

[S6]. Jiang, J.X., Chen, X., Fukada, H., Serizawa, N., Devaraj, S., and Torok, N.J. (2013). Advanced glycation endproducts induce fibrogenic activity in nonalcoholic steatohepatitis by modulating TNF-alpha-converting enzyme activity in mice. Hepatology *58*, 1339-1348. 10.1002/hep.26491.

[S7]. Najjar, S.M., Ledford, K.J., Abdallah, S.L., Paus, A., Russo, L., Kaw, M.K., Ramakrishnan, S.K., Muturi, H.T., Raphael, C.K., Lester, S.G., et al. (2013). Ceacam1 deletion causes vascular alterations in large vessels. Am J Physiol Endocrinol Metab *305*, E519-529. 10.1152/ajpendo.00266.2013.

[S8]. Yoo, J.Y., Cha, D.R., Kim, B., An, E.J., Lee, S.R., Cha, J.J., Kang, Y.S., Ghee, J.Y., Han, J.Y., and Bae, Y.S. (2020). LPS-Induced Acute Kidney Injury Is Mediated by Nox4-SH3YL1. Cell Rep *33*, 108245. 10.1016/j.celrep.2020.108245.